Symbolic Translation of the Spatial Imagery of Fuzhou Ancient Houses and Its Driving Effect on Textile Industry Product Design

Xiang Huang
School of Art and Design, Fuzhou Technology and Business University, Fuzhou 350715, Fujian, China
Corresponding author: Xiang Huang (e-mail: m15505906302_1@163.com)

ABSTRACT Architectural cultural heritage contains abundant geometric and chromatic information that can be systematically transformed into industrial design resources through computational modeling. This study proposes a semantic graph-based symbolic translation framework for converting the spatial imagery of Fuzhou ancient houses into textile product design elements. First, geometric contours are extracted using Canny edge detection and the Douglas–Peucker algorithm, while dominant color distributions are quantified in HSV space. A multi-layer semantic graph is then constructed from roof curvature, geometric proportions, symmetry characteristics, and color relationships. Node2Vec embedding and graph convolutional networks are subsequently employed to generate stable symbol vectors, which are further transformed into textile pattern matrices through frequency-domain texture synthesis based on fast Fourier transforms and parameterized repeating units. Experimental results demonstrate that the proposed framework achieves high symbolic stability and reliable color reproduction while maintaining satisfactory manufacturability for textile applications. Beyond regional cultural preservation, the combination of graph representation learning and frequency-domain pattern generation provides a computational paradigm for structured visual information encoding and periodic pattern synthesis. Such characteristics offer methodological references for digital design problems involving electromagnetic-inspired periodic structures, antenna surface pattern optimization, and intelligent engineering systems requiring spatial feature representation and frequency-domain analysis.

INDEX TERMS semantic graph, symbolic translation, frequency-domain analysis, textile pattern generation, spatial imagery

I. INTRODUCTION

FUZHOU ancient houses are key carriers of Fujian culture, as their architectural forms, decorative symbols, and materials embody distinct historical and aesthetic logics, reflecting both residential functions and regional social order [1,2]. Existing studies have mainly focused on contextual interpretation, preservation, and reuse, with limited attention to translating spatial imagery into a unified symbolic system [3,4]. This limitation hinders the construction of architectural cultural elements suitable for industrial production. Textile design relies on stable symbolic systems, yet most prior research remains at the level of image description or artistic reproduction, lacking a complete translation mechanism [5,6]. The spatial richness of ancient houses raises three challenges: simplified geometric extraction of form [7,8], subjective color derivation without parametric indicators [9,10], and limited symbol vectorization that cannot be effectively linked to textile standards. Consequently, the transferability and regenerative potential of architectural culture in industrial design are weakened, highlighting the need for a systematic symbolic translation path from ancient house imagery to textile design language.

In studies of architectural cultural symbols, scholars have examined the cultural meanings and regional characteristics of architectural elements. Wang et al. analyzed the relationship between religious building facades in Jingzhou and social order using semantic methods [11], while Ma et al. revealed the Confucian core and diversified integration of academy decorations through diversity indices and social network analysis [12]. Song and Liao noted that Jiangxi traditional architecture developed a simple and practical style under multiple influences [13]. From a cross-cultural perspective, AI Dein applied semiotics to Islamic architectural elements and proposed paths for contemporary innovation based on traditional symbols [14]. Although these studies clarify the multidimensional links between architectural symbols and regional culture, they remain limited in comparing symbolic mechanisms and in systematically applying symbolic principles to textile design [15,16].

In studies on symbol translation and textile design, Ren et al. applied Morris semiotics to construct a ski-suit symbol translation model integrating regional culture and function [17]. Cong et al. analyzed textile trademarks from the Republic of China to reveal national spirit and historical connotations [18], while Ampadu et al. introduced traditional West African symbols into textile design to test their applicability [19]. Despite these contributions, existing studies remain limited in multidisciplinary integration and in their linkage to industrialization.

To address these issues, this study proposes a semantic graph-based symbolic translation approach. Geometric outlines are simplified using the Canny operator and the Douglas–Peucker algorithm, while dominant colors are decomposed numerically through HSV space and K-means clustering. A multilevel semantic graph is then constructed from roof curvature, proportions, symmetry, and color distribution, with features aggregated using Node2Vec and graph convolutional networks. The resulting embeddings are converted into textile patterns via fast Fourier transform–based parameterized repeating units, enabling industrial application. This framework achieves a complete pipeline from architectural imagery to textile symbols, integrating symbol abstraction, semantic modeling, and pattern generation, while balancing computational structure with design expression through both quantitative evaluation and visual description.

II. SYMBOLIC TRANSLATION OF THE SPATIAL IMAGERY OF FUZHOU ANCIENT HOUSES

A. EXTRACTION OF SPATIAL MORPHOLOGY AND COLOR FEATURES OF ANCIENT HOUSES

The spatial imagery of Fuzhou ancient houses is primarily composed of geometric forms and color relationships. The first step in its symbolic translation is to quantify these forms and colors.

For morphological feature extraction, the Canny algorithm is used to extract edge contours of roofs, eaves, window lattices, and other structures. If the horizontal and vertical gradient components of the image are denoted by G_x and G_y, respectively, the gradient amplitude is defined as:

$$M = \sqrt{G_x^2 + G_y^2} \tag{1}$$

Threshold filtering is used to obtain a relatively complete set of edges. To further reduce redundancy and obtain recognizable contour units, the Douglas–Peucker algorithm is applied to perform polygonal approximation on the boundary curves, making the morphological representation more concise. For color feature extraction, RGB is converted to HSV color space, and the calculation of hue H, saturation S, and value V followed standard formulas. K-means clustering is then used to classify the pixels, with the optimization objective being:

$$J = \sum_{i=1}^{k} \sum_{x \in C_i} \|x - \mu_i\|^2 \tag{2}$$

In Formula (2), μ_i is the cluster center vector, and the ratio within the cluster reflects the proportion of the color tone. Therefore, the main and secondary colors of the ancient house can be extracted.

Finally, the geometric contour unit and the color parameter vector together constitute the primary quantitative set of the spatial image of the ancient house, laying the data foundation for subsequent semantic modeling and symbol embedding. This study analyzes the relationship between architectural spatial form and color in the feature extraction and semantic modeling stages based on repeatable numerical indicators and structural parameters. Relevant spatial features are quantitatively described using edge density, curvature distribution, color proportion, and saliency indicators. Since the research focuses on symbolic abstraction and semantic embedding mechanisms, rather than image recognition or visual reproduction itself, the architectural visual features relied upon in the analysis are expressed through parametric description and numerical statistics, thereby ensuring that the subsequent semantic graph construction and symbol vector embedding are based on a clear spatial and color logic.

To construct a perceptually grounded quantitative system, two metrics—Feature Saliency and Prominence— were introduced to link geometric and visual attributes. Feature Saliency was defined by local luminance and gradient contrast within architectural subregions, computed from the Canny edge map using normalized differences between local and mean luminance and gradient magnitude. Prominence was defined as the normalized product of edge density and average curvature, where edge density represents the proportion of edge pixels and curvature is derived from Douglas–Peucker–approximated contours. Together, these metrics extend purely geometric measures by incorporating perceptual visibility and structural emphasis, ensuring that visual attention evaluation is based on reproducible computational formulations rather than subjective judgment.

B. SPATIAL IMAGE SEMANTIC GRAPH MODELING

In addition to the descriptive quantitative results involving form and color, it is also necessary to construct a semantic graph model to describe the internal structure of the spatial image of the ancient house. The semantic labelling system is generally based on four key parameters: the curvature of the roof, the geometric grid ratio, the position of the symmetry axis, and the ratio of color.

Curvature of the roof: generated points were obtained using the average curvature parameter, which is calculated by using discrete second-order derivative approximations of the contour curve to describe the curvature of the roof.

Geometric grid ratio: describes the geometric division characteristic by the local side length as a ratio to the overall boundary length.

Symmetry axis position: describes overall symmetry through distribution of the main axis using the geometric center as the benchmark.

Color ratio: measured according to the clustering results and calculated based on comparisons of the ratio of the number of pixels with different hues relative to the total number of pixels.

To ensure accurate correspondence between geometric and chromatic properties, semantic graph nodes were refined to represent roof or facade subregions generated through joint spatial–color partitioning. Each node defines a bounded region, enabling simultaneous measurement of local curvature, grid ratio, symmetry deviation, and average color ratio. Structural descriptors are extracted from edge-based maps, while color ratios are computed from pixels within the same region. This co-located sampling ensures that geometric and chromatic attributes originate from an identical physical area, forming a unified node feature vector.

$$x_i = (k, r, s, c) \tag{3}$$

The inclusion of color ratio within the node feature does not imply equivalence between global and local attributes. Here, color ratio denotes the normalized proportion of dominant colors within each segmented node area, ensuring scale consistency with geometric attributes. This enables joint encoding of local structural variation and color tendency within a unified node-based representation. In Formula (3), curvature is denoted by k, grid ratio by r, symmetry position by s, and color ratio by c.

The adjacency matrix encodes both geometric adjacency and color contrast between nodes and is normalized to form a semantic graph. This graph integrates local morphological and chromatic features while capturing their logical relationships, providing a foundation for symbolic abstraction.

C. SYMBOL EMBEDDING AND ABSTRACTION MECHANISM

Based on the semantic graph, it is necessary to map node features to low-dimensional vectors to form a stable symbolic expression. For this purpose, two methods, Node2Vec and Graph Convolutional Network (GCN), are applied.

Node2Vec operates by sampling node sequences through biased random walk, maximizing the conditional probability between a node and its contextual neighbors to obtain the embedding vector:

$$\max \sum_{u \in V} \log P\left(N(u) \mid f(u)\right) \tag{4}$$

In Formula (4), $f(u)$ represents the embedding representation of node u, and $N(u)$ denotes its neighbor set.

GCN aggregation is then applied after the initial embedding to achieve feature aggregation and hierarchical abstraction. Its propagation rule is:

$$H^{(l+1)} = \sigma\left(\tilde{A} H^{(l)} W^{(l)}\right) \tag{5}$$

Unlike previous approaches, Node2Vec and GCN are not applied in parallel or treated as redundant layers. Instead, Node2Vec functions as a probabilistic structural encoder, learning embeddings that capture contextual proximity through biased random walks and preserve local co-occurrence among architectural components. The resulting embeddings initialize the feature space, maintaining both spatial adjacency and high feature similarity.

The GCN treats Node2Vec embeddings as structured priors and applies layered transformations to extract hierarchical correlations while suppressing noise from irrelevant contextual links. This design combines local continuity with global coherence, as Node2Vec regularizes the input representation and reduces sensitivity to graph topological fluctuations. Building on this stable feature basis, GCN performs topological learning to refine embeddings into semantically balanced representations that support reproducible symbol generation. In Formula (5), $\tilde{A}$ is the normalized adjacency matrix; $W^{(l)}$ is the learnable weight; σ is the activation function. Two outputs are produced through consecutive stages of embedding and aggregation. The first, $f(u)$, is generated by Node2Vec via biased random walks on the semantic graph, encoding local contextual relationships as low-dimensional vectors. The second, $H^{(l+1)}$, results from subsequent graph convolution, aggregating neighborhood information to refine relationships among curvature, grid ratio, symmetry, and color proportion within a unified embedding space. By combining Node2Vec's local structural encoding with GCN's global feature aggregation, node information is transformed into a hierarchical and stable set of symbol vectors. This stable set corresponds to the converged $H^{(l+1)}$ vectors, each representing a semantic node with integrated latent attributes in a fixed-dimensional space. Stability is verified through convergence tests using intra-class variance and silhouette coefficients, ensuring consistency across training runs. This structured representation improves interpretability and serves as the final dataset for subsequent symbolic translation and textile pattern generation.

D. TRANSLATION FROM SYMBOL VECTORS TO PATTERNS

Once the stable set of symbol vectors is trained, we transform them into a two-dimensional pattern representation for further textile design. This can be done in two ways: frequency domain synthesis and unit division.

The set of symbol vectors learned from semantic embedding is arranged into a structured two-dimensional feature matrix before the frequency-domain transformation. Each node vector (k, r, s, c) is projected into a scalar intensity value through weighted fusion $v_i = \alpha k_i + \beta r_i + \gamma s_i + \delta c_i$, where the weights α, β, γ, δ are normalized coefficients computed by the variance ratio of the four features from all node vectors. This operation not only maintains the relative influence of geometric and chromatic attributes but also converts the high-dimensional symbol representation into a uniform scalar field. Then the set $\{v_i\}$ is spatially arranged according to the adjacency order of the semantic graph. Finally, a two-dimensional symbol intensity map is formed with both local connectivity and hierarchical abstraction.

The constructed two-dimensional pattern representation is further transformed to the frequency domain with two-dimensional Fast Fourier Transform (2D-FFT).

$$F(u,v)=\sum_{x=0}^{M-1}\sum_{y=0}^{N-1} I(x,y)e^{-j2\pi\left(\frac{ux}{M}+\frac{vy}{N}\right)} \tag{6}$$

The variables x and y denote the spatial coordinates of the two-dimensional symbol intensity map, while u and v correspond to the frequency components along the horizontal and vertical directions, respectively, ensuring that spatial periodicity and directional texture characteristics are simultaneously encoded in the frequency domain. The 2D Fourier transform decomposes the spatial distribution of symbol intensities into horizontal and vertical frequency components, preserving structural periodicity while revealing dominant texture rhythms. Using 2D-FFT, rather than 1D-FFT, ensures compatibility with the planar pattern matrix and the continuous numerical field generated by weighted symbol fusion. This establishes a direct mathematical link between multidimensional symbolic data and spatial frequency representation. Amplitude and phase are adjusted in the frequency domain to maintain continuity and layering, followed by an inverse transform to produce the base symbol texture.

Next, to meet the regularity requirements of textile craftsmanship, the pattern is parameterized and divided into units. Assuming that the primitive function is $p(x,y)$, and the horizontal and vertical step sizes are Δx and Δy, the overall pattern matrix can be expressed as:

$$P(x,y)=\sum_{m=0}^{M-1}\sum_{n=0}^{N-1} p(x-m\Delta x, y-n\Delta y) \tag{7}$$

By adjusting the repetition method, pattern matrices with translational, mirror, or rotational symmetry can be generated, thereby ensuring the periodicity and structural regularity of the pattern while facilitating the formation of regular and continuous pattern configurations that conform to subsequent weaving constraints. In summary, the FFT provides a mechanism for generating continuous and periodically structured textures at the pattern level, while the parameterized unit partition enforces spatial regularity within the pattern matrix. Together, these operations establish a mathematically stable and visually coherent pattern framework that is compatible with textile manufacturing constraints, which are explicitly addressed and validated at the process-mapping stage described in the subsequent section.

E. MAPPING OF TEXTILE INDUSTRY PRODUCT DESIGN

After generating a regular pattern matrix, it is mapped onto fabric structures to enable industrial textile application. This study couples symbol sets with textile process parameters as the structural basis of the mapping. Let M denote the pattern matrix, whose grayscale or color values correspond to warp–weft weaving units. The process mapping function is then defined accordingly.

$$T=f(M,P) \tag{8}$$

In Formula (8), the parameter set includes warp and weft density, weaving point distribution, and yarn material, along with constraint thresholds defined by established industrial weaving practices rather than the symbolic translation model itself. These constraints follow widely adopted loom specifications and textile engineering standards, such as limits on float length, maximum thread count, and warp–weft tension ratio to ensure production feasibility. The process suitability coefficient, S_p, is calculated as the weighted ratio of suitable parameters to the total number of parameters across all symbolic units.

Here, a positive instance denotes a process parameter whose mapped numerical value lies fully within the admissible operational range defined by industrial weaving constraints. These ranges are specified by established textile engineering standards rather than the symbolic model itself. A parameter is considered positive only when all feasibility conditions are strictly satisfied, ensuring that the evaluation reflects manufacturability rather than aesthetic or design preference.

The weighting scheme for S_p follows the same normalization principle used in symbol-to-pattern fusion, assigning each process parameter a contribution proportional to its variance across the symbolic dataset. Parameters with higher sensitivity to pattern variation thus exert greater influence, while less variable parameters contribute less. Weights are computed globally rather than per unit, ensuring consistent evaluation across pattern instances.

Thus, the final Process Suitability score is calculated as the normalized average of S_p across all pattern units, providing quantitative validation of industrial manufacturability under standard conditions and confirming the full industrial applicability of the symbolic translation process.

The current definition of S_p is limited to the material systems and loom configurations specified by the referenced industrial standards. Although the evaluation framework is structurally transferable, numerical thresholds and admissible ranges are context dependent. Therefore, cross-material or cross-loom application requires recalibration of feasibility boundaries, and suitability results should be interpreted within the defined industrial context.

With this function, each symbolic unit of a pattern is transferred into a unit of fabric structure to ensure the visual effect is reasonable from the process suitability perspective.

Although S_p is computed at the level of individual symbolic units, the reported process suitability values represent an aggregated assessment across the entire pattern matrix. Each symbolic unit is evaluated independently against the same global parameter constraints, and the final suitability score reflects the collective feasibility of all units under a unified industrial context rather than isolated local compliance. Therefore, the numerical thresholds applied in the process mapping stage function as feasibility constraints rather than optimization targets, ensuring that the generated symbolic patterns remain compatible with realistic industrial weaving conditions instead of defining design-driven parameter optima.

In addition, the symbol set can be classified into two categories: color symbols and geometric symbols. Color symbols correspond to color yarn ratio, whereas geometric symbols correspond to weaving structure parameters.

Then, the two types of symbols are coupled with process parameters, and the bidirectional relationship between symbolic patterns and production parameters is constructed, so that the symbolic patterns of Fuzhou ancient houses can be implemented and transformed into textile products with regional culture.

III. SYMBOLIC TRANSLATION RESULTS AND TEXTILE DESIGN VERIFICATION

A. RESULTS ON THE SPATIAL FORM AND COLOR CHARACTERISTICS OF ANCIENT HOUSES

It should be noted that all spatial density, proportion, and salience indicators reported in this study are derived from normalized image representations rather than calibrated physical measurements. No camera parameters, shooting distance, or surveying references were introduced to establish a correspondence between pixel dimensions and real-world metric units. Consequently, the reported density values describe relative structural concentration within the image domain and serve the purpose of symbolic comparison and semantic abstraction, rather than physical quantification of architectural elements. This study analyzes the spatial imagery of ancient houses by examining the distribution and visual features of architectural parts using multidimensional edge-detection statistics, including edge length ratio and edge density. These measures describe global and local geometric distributions, while curvature and salience characterize morphological complexity and visual prominence. Based on these results, quantitative and perceptual evaluation indices are constructed, with experimental outcomes shown in Figure 1.

The analyzed visuals include façade, roof, eave, and window lattice images of selected Fuzhou old houses. All images were normalized in resolution, luminance, and color to ensure consistent feature extraction. Key environmental characteristics include arched roof contours, dense modular lattice grids, and a dominant palette of blue-gray and ochre-red complemented by wood brown and ink black.

To ensure that the evaluation of architectural components in Figure 1 and Figure 2 is objective and reproducible, the quantitative indices Prominence and Visual Salience were calculated using explicit formulas. Prominence was defined as the normalized product of edge density and mean curvature of each component, expressed as:

$$P_i = \frac{E_i \times C_i}{\sum_{j=1}^{n} E_j \times C_j} \tag{9}$$

where E_i represents the edge density of component i obtained through the Canny edge map, defined as the ratio between the number of detected edge pixels and the total pixel area of the corresponding component region in the normalized image domain, and C_i is the average curvature derived from the contour curve of that component. Visual Salience was determined from the normalized luminance and gradient contrast of each region in the image, calculated as:

$$S_i = \frac{1}{m_i}\sum_{p=1}^{m_i}\left(\frac{|G_p|}{\max(G)} + \frac{|L_p - \bar{L}|}{\bar{L}}\right) \tag{10}$$

where $|G_p|$ denotes the gradient magnitude at pixel p, L_p denotes its luminance, and $\bar{L}$ is the mean luminance of the image. All architectural element images were standardized to 256 $\times$ 256 pixels to ensure comparability. All subsequent geometric and density-related indicators are therefore computed within a normalized image coordinate system and do not correspond to absolute physical dimensions, and the calculations were implemented in MATLAB 2024b. The resulting values provide consistent numerical support for the structural prominence and visual perception of each architectural component.

Figure 1 shows that the edge length of the roof line accounts for 25.8%, and the normalized edge density is 14.2 per unit image area, indicating that it occupies a dominant position in the overall composition and maintains a high concentration. The edge length of the window lattice line accounts for 13.4%, but the density reaches 18.9 per unit image area, reflecting that although the proportion is limited, it presents a local high-density feature due to the complexity of the lines. The edge length of the ridge decoration accounts for only 3.7%, with a density of 5.8 per unit image area, but the curvature value is 0.72, and the significance is 0.84, indicating that although the number of such elements is small, they produce a prominent effect in visual perception through high curvature and strong gradient. The edge length of the eaves edge is 15.6%, with a density of 10.7 per unit image area, a curvature value of 0.55, and a significance value of 0.86. This balance indicates that the load-bearing and enclosing parts of the structure form the spatial framework using proportion and density, while the decorative part produces a visual effect through the degree of geometric complexity and prominence. These two characteristics combined constitute the hierarchy of the image of space in ancient houses.

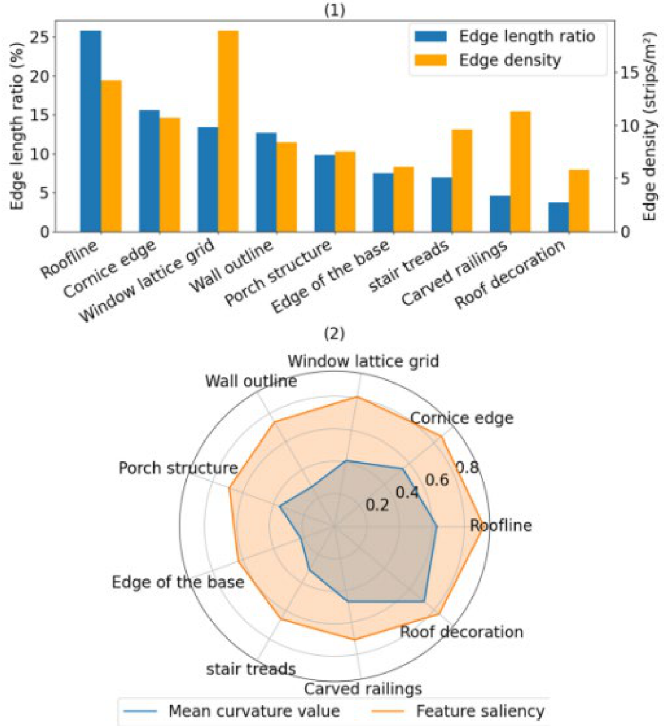

FIGURE 1. Multi-dimensional feature distribution analysis of edge detection in ancient houses. (1) Spatial features; (2) Visual form

Color analysis is essential for capturing the overall visual tone and decorative level of ancient houses. Focusing on primary and secondary color proportions, rather than hue and saturation alone, better reflects architectural color composition. Using HSV-based clustering, this study quantifies color proportions alongside perceptual attributes such as salience, brightness, and saturation. These measures describe both the spatial coverage and visual intensity of dominant colors, forming a consistent quantitative representation of architectural color distribution aligned with Figure 2. This integrated system supports subsequent symbolic analysis by linking overall hue to local decorative effects.

All salience and prominence values in Figure 2 were computed using the quantitative definitions in Section “Results on the Spatial Form and Color Characteristics of Ancient Houses” and are reproducible. Blue-gray is dominant (32.7%, salience 77.8%), stabilizing the roof-based color scheme, while ochre red accounts for 26.4% with higher salience (81.6%), producing strong visual impact on walls due to its high brightness and saturation. Wood brown (16.8%, salience 66.2%) functions as a harmonizing color for doors, windows, and beams, whereas dark black (9.1%, prominence 70.7%) creates strong outlines despite limited area. Off-white and other colors together account for about 15% with lower prominence and serve as background tones. Overall, blue-gray and ochre red form the dominant palette, complemented by wood brown, dark black, and off-white to produce a heavy and profound spatial image.

B. SPATIAL SEMANTIC MAP AND SYMBOL EMBEDDING RESULTS

In semantic map construction, four key spatial features of Fuzhou ancient houses are statistically analyzed: roof curvature coverage, mean and standard deviation of geometric grid ratio, symmetry axis position, and mean and standard deviation of color ratio. The stability and balance of local semantic labels are evaluated using coverage, node mean, standard deviation, and information entropy, providing reliable parameters for subsequent symbol embedding and vector abstraction. Statistical results are shown in Figure 3.

Figure 3 indicates high and balanced coverage across all semantic features. Roof curvature shows the highest coverage (0.94) with moderate variation (mean 0.57, SD 0.22), reflecting widespread yet variable morphological complexity. Geometric grid ratio coverage is 0.85, with a low mean (0.43) and relatively high entropy (1.12), indicating generally small but evenly distributed spatial divisions. Symmetry axis coverage reaches 0.90 (mean 0.54, SD 0.28), suggesting overall axial symmetry with local variation. Color proportion coverage is 0.87, with a higher mean (0.63), low variation (SD 0.16), and high entropy (0.88), indicating stable yet diverse color distribution. Together, these results demonstrate strong consistency and balance among semantic labels, supporting reliable symbol embedding.

After finishing the statistical analysis of semantic label distribution, we also cluster the symbol vector by Node2Vec embedding and analyze the separation and stability of

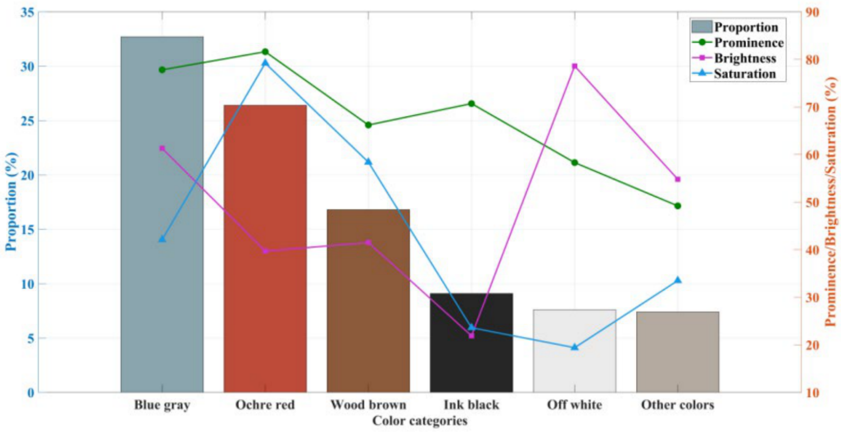

FIGURE 2. Distribution and characteristic analysis of primary and secondary colors in Fuzhou ancient houses

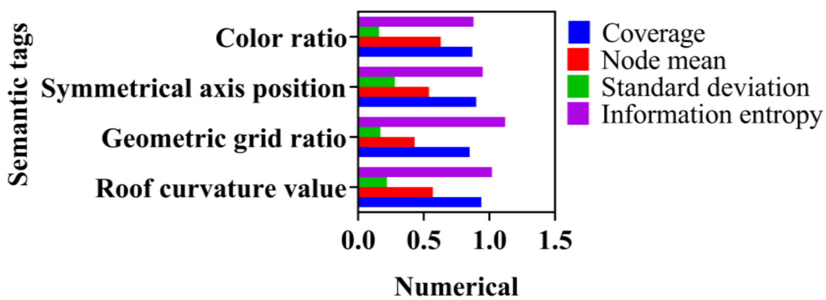

FIGURE 3. Statistical results of semantic label distribution for spatial imagery of Fuzhou ancient houses

different semantic feature in distribution after embedding. Intra-class average distance, inter-class average distance, intra-class variance and silhouette coefficient are used to quantitatively assess clustering performance after embedding, revealing the aggregation density and discrimination capability of different features in the low-dimensional space, as shown in Figure 4.

Figure 4 shows the classification evaluation metrics for the four semantic features. The average intra-class distance, intra-class variance, and silhouette coefficient of the symmetric cluster are 0.16, 0.06, and 0.71, respectively, indicating that the vector distribution of symmetric clusters is more concentrated and the boundaries are clearer, which is consistent with the stable axial symmetry of ancient building structures. The average intra-class distance, average inter-class distance, and silhouette coefficient of the curvature-dominated class are 0.18, 0.62, and 0.64, respectively, indicating that curvature features have high discriminative power and numerical volatility. The average intra-class distance and average inter-class distance of the grid-related class are 0.21 and 0.59, respectively; the corresponding silhouette coefficient reaches 0.58, which reflects a moderate level of clustering separation. Compared with the symmetry- and curvature-dominated classes, the grid-related features exhibit relatively weaker spatial partitioning and more blurred boundaries among local samples, indicating that geometric grid attributes show higher internal variability in the embedded space rather than a failure of clustering. The average intra-class distance and average inter-class distance of the color-dominated class are 0.19 and 0.61, respectively; therefore, the silhouette coefficient of this class is 0.63, indicating that the colors of ancient buildings have a high degree of concentration overall, and the boundary separation is weaker than that of symmetric features.

C. PATTERN GENERATION AND REGULARITY

In the pattern synthesis stage, symbol vectors are transformed into the frequency domain using FFT to analyze energy distribution. The amplitude intensity, power spectrum and cumulative energy ratio across frequency indices are then examined. The simulation results demonstrate that the method identifies dominant frequencies and energy concentration range, forming the basis for pattern generation and regularity verification. Although the frequency transformation is performed in a two-dimensional spectral space, the dominant frequency characteristics are summarized through an aggregated frequency representation to facilitate quantitative analysis and visualization. The resulting frequency spectrum is shown in Figure 5.

As shown in Figure 5, when $\omega = 0.25$, the amplitude

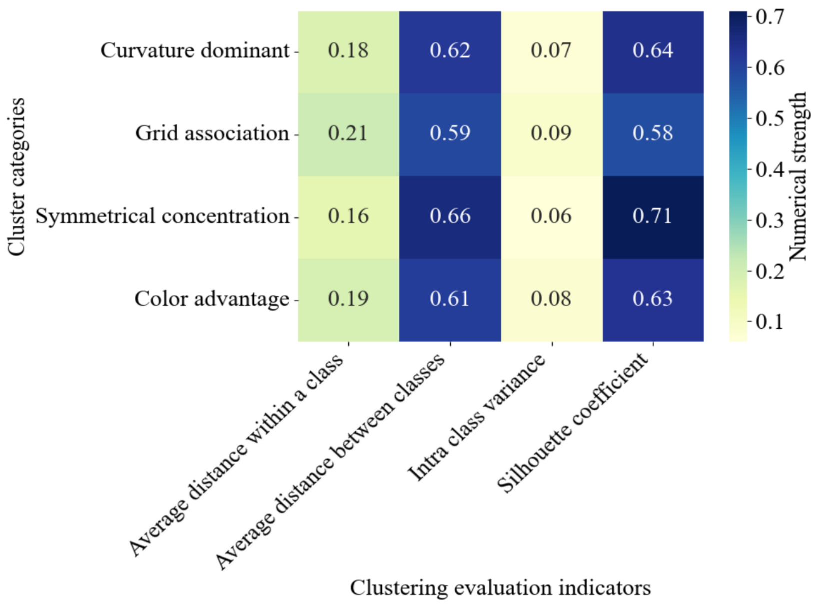

FIGURE 4. Heatmap of symbolic vector clustering after Node2Vec embedding

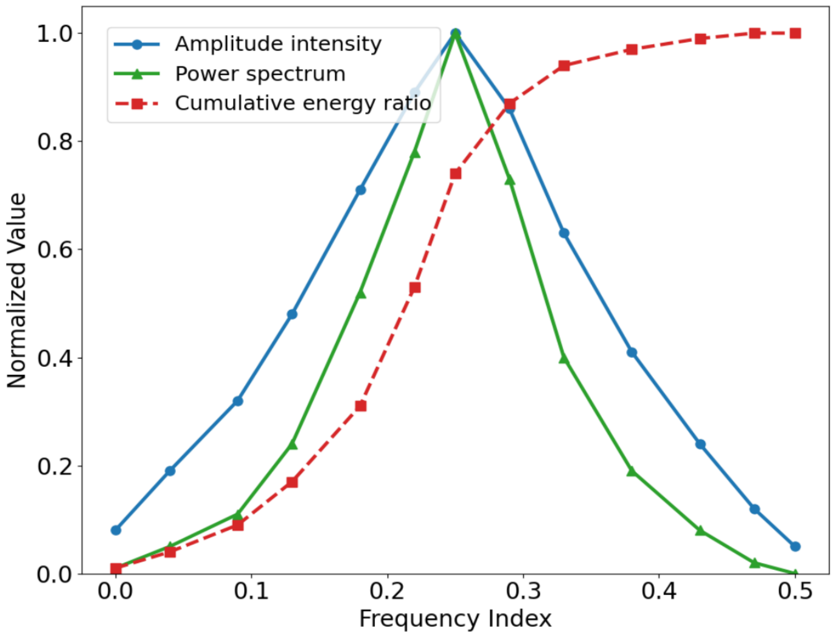

FIGURE 5. Aggregated frequency spectrum and energy distribution derived from the two-dimensional Fourier spectrum of the symbol intensity matrix

intensity and power spectrum both reach 1.00, while the cumulative energy ratio is 0.74, indicating that most of the pattern energy is concentrated in the mid-frequency range and primarily located at the dominant peak. In the low-frequency area, between the frequency index of 0.09 and 0.13, the amplitude increases from 0.32 to 0.48; the power spectrum increases from 0.11 to 0.24; the cumulative energy ratio is 0.17, which means that the low-frequency component takes up a very small amount of energy, but it is important for structure. As frequency increases, the amplitude decreases to 0.86 at 0.29; the power spectrum reaches 0.73; the cumulative energy ratio increases to 0.87, indicating that energy rapidly accumulates after the mid-frequency range and approaches saturation. Amplitude gradually decreases in the high-frequency range and is only 0.12 at 0.47, which corresponds to a power spectrum of 0.02 and a cumulative energy ratio of about 1.00, indicating a poor dispersion of high-frequency energy and a very small proportion. In general, clearly defined bands of energy concentration and decay are observed. The spectrum is continuous and suitable for weaving.

Furthermore, the visual characteristics observed in the generated textile patterns correspond to the dominant structural attributes encoded in the symbol vectors derived from the semantic graph. Patterns associated with curvature-related vectors exhibit continuous directional variation consistent with the mid-frequency energy concentration identified in the spectral analysis, while grid-related vectors give rise to repeated orthogonal arrangements reflecting the regular spacing encoded in the adjacency structure. Symmetry-axis vectors produce balanced bilateral configurations aligned with the stability of axial distribution measured in the embedding space, and color-ratio vectors manifest layered chromatic transitions that are coherent with the proportional color parameters embedded in the node features. These descriptions serve to interpret the structural implications of the quantitative frequency-domain results rather than constituting independent evaluative evidence.

D. TEXTILE PRODUCT DESIGN VERIFICATION

In the field of pattern design generalization, taking six aspects of symbol stability, color reproduction, continuity pattern, craft adaptability, prominent display and comprehensive adaptability as evaluation indexes, the quantitative patterns of different types are statistically measured and compared in order to analyze and study the multiple index level performance of the pattern in different types. The roof curvature pattern, geometric grid pattern, symmetrical axis pattern and color-ratio pattern are selected as the research objects, and the comparative analysis of balance and prominence of different patterns in different attributes is carried out in the same evaluation system. At last, in order to intuitively show the evaluation results of multi-dimensional evaluation, the pattern index scatter plot is constructed.

Figure 6 shows the distribution features of different patterns in different directions. The roof curvature pattern obtains the highest visual salience score of 0.91, while its process adaptability score is 0.81. The geometric grid pattern has relatively balanced form advantage and process adaptability with symbol stability score of 0.91 and process adaptability score of 0.87. The symmetrical axis pattern has the highest symbol stability score of 0.93, while its color reproduction score is the second highest and is 0.83. The pattern has a clear advantage in term of form standardization and a disadvantage in color expression. The color ratio pattern has the highest color reproduction score of 0.90 and its visual salience score is 0.93. The pattern has a clear advantage in color expression and its symbol stability score is slightly lower than the other patterns and is 0.87. In general, the different patterns have different advantages in symbol, color and process.

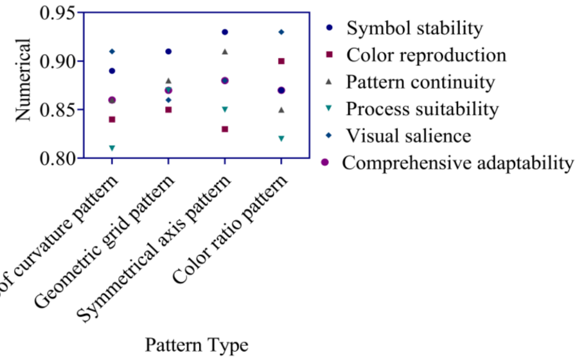

FIGURE 6. Compatibility index of symbolic patterns embedded in textile products

The qualitative labels show good agreement with the respective measured indices. The curvature pattern matches the rhythmic profile of the roof, the grid pattern matches the modular structure of lattice work, the symmetry pattern matches the symmetry of conventional designs, and the color-ratio pattern matches the contrast harmony of conventional designs. These results suggest that the symbolic translation method is computationally feasible and perceptually coherent.

The descriptive interpretation complements the quantitative validation of the symbolic matrix. Form and tone are verbally reconstructed to demonstrate the aesthetic coherence between Fuzhou ancient houses and the generated textile structures. The symbolic translation pathway is thus shown to be technically and perceptually effective.

IV. CONCLUSIONS

This paper proposes a semantic graph-based symbolic translation framework that converts the geometric and chromatic features of Fuzhou ancient houses into computable symbols for textile design. By integrating Node2Vec and graph convolutional networks, the method achieves vectorized abstraction, while FFT-based frequency synthesis and parametric unit partition generate regular pattern matrices, forming a complete technical chain from architectural imagery to textile language. Experimental results demonstrate the effectiveness of the approach, including the dominance of roof geometry (25.8% edge length, density 14.2), the stability of blue-gray as a primary color (32.7%, salience 77.8%), and strong semantic embedding performance (silhouette coefficient 0.71). These findings confirm the reliability of symbol extraction, semantic stabilization, and pattern generation for integrating regional culture into textile design. The study is subject to limitations related to sample scope, regional diversity, and incomplete exploration of weaving parameters with novel materials, which constrain generalizability. The reported stability reflects intra-sample consistency rather than cross-regional robustness. Future work will extend the framework to ancient residential architectures across different regions and typologies to evaluate its universality. In addition, comparative analysis reveals a trade-off between structural stability and color fidelity within the current framework, stemming from the coupling behavior of Node2Vec–GCN embeddings. Future research will address this by adjusting node feature weights and aggregation strategies to better balance structural coherence and chromatic reproduction in symbolic textile translation.

AUTHOR CONTRIBUTIONS

Xiang Huang designed, collected and analyzed the data, and drafted the manuscript. Xiang Huang conducted the study, critically revised the manuscript for important intellectual content, and gave final approval of the version to be published. Xiang Huang participated fully in the work, take public responsibility for appropriate portions of the content, and agreed to be accountable for all aspects of the work in ensuring that questions related to the accuracy or integrity of any part of the work are appropriately investigated and resolved.

CONFLICTS OF INTEREST

The author declares no conflict of interest.

FUNDING

This research was funded by,

1. FJ2023C065 2023 Fujian Social Science Fund Project "Research on the Revitalization of Cultural Heritage through Visual Narrative of Fuzhou Ancient Houses from the Perspective of Cultural Consciousness".

2. 2025 Fuzhou Social Science Fund Project. Research on the Protection, Activation and Utilization of Fuzhou Traditional Cultural Blocks, Ancient Villages and Ancient Buildings Based on the Cultural Landscape Gene

Theory. Project No.: 2025FZC118

ACKNOWLEDGEMENTS

Not applicable.

REFERENCES

[1] J. Zhang, L. Jiang, X. Wang, Z. Chen, and S. Xu, "A study on the spatiotemporal aggregation and corridor distribution characteristics of cultural heritage: the case of Fuzhou, China," Buildings, vol. 14, no. 1, pp. 121, 2024, doi: 10.3390/buildings14010121.

[2] L. Huang, S. Liu, and Z. Kang, "The Protection of Urban Spatial Structures in Historic Cities: A Multi-Actor Perspective of the Cultural Space Construction in Fuzhou, China," Sustainability, vol. 16, no. 1, pp. 385, 2023, doi: 10.3390/su16010385.

[3] L. Wu, D. Cao, J. Yang, R. Zhang, and X. Yan, "The Symbolization of Regional Elements Based on Local-Chronicle Text Mining and Image-Feature Extraction," ISPRS International Journal of Geo-Information, vol. 13, no. 9, pp. 299, 2024, doi: 10.3390/ijgi13090299.

[4] J. Wang, Y. Shi, W. Xu, and Y. Wu, "Identification of Spatial and Symbolic City Image Elements Through Social Media Data: A Case Study of Hangzhou," Land, vol. 13, no. 12, pp. 2194, 2024, doi: 10.3390/land13122194.

[5] N. Patel, "The impact of architecture embellishment on traditional motifs: a study," International Journal for Research in Applied Science and Engineering Technology, vol. 10, no. 12, pp. 1766-1773, 2022, doi: 10.22214/ijraset.2022.48300.

[6] S. ul Saba, S. Rafique, F. Tauqeer, and I. Seemi, "Innovative Textile Desiging for Ladies Apparels from Architectural Motifs of Sethi House," Pakistan Journal of Humanities and Social Sciences, vol. 11, no. 2, pp. 1666-1675, 2023, doi: 10.52131/pjhss.2023.1102.0471.

[7] Q. Li, L. Mou, Y. Sun, Y. Hua, Y. Shi, and X. X. Zhu, "A review of building extraction from remote sensing imagery: Geometrical structures and semantic attributes," IEEE Transactions on Geoscience and Remote Sensing, vol. 62, pp. 1-15, 2024, doi: 10.1109/TGRS.2024.3369723.

[8] Y. Chen and W. Yao, "Extraction of orthogonal building boundary from airborne lidar data based on feature dimension reduction," ISPRS Annals of the Photogrammetry, Remote Sensing and Spatial Information Sciences, vol. 2, pp. 351-358, 2022, doi: 10.5194/isprs-annals-V-2-2022-351-2022.

[9] P. Flores-Vidal, D. Gómez, J. Castro, and J. Montero, "New aggregation approaches with HSV to color edge detection," International Journal of Computational Intelligence Systems, vol. 15, no. 1, pp. 78, 2022, doi: 10.1007/s44196-022-00137-x.

[10] L. Zhang, Y. Zhang, Y. Wei, T. Zhang, J. Zhang, and J. Xu, "Unveiling Patterns and Colors in Architectural Paintings: An Analysis by K-Means++ Clustering and Color Ratio Analysis," Tehnički vjesnik, vol. 30, no. 6, pp. 1870-1879, 2023, doi: 10.17559/TV-20230514000634.

[11] G. Wang, W. Huang, and Q. Xu, "Constructing a Semantic System of Facade Elements for Religious Architecture from a Regional Perspective: A Case Study of Jingzhou," Buildings (2075-5309), pp. 14(10), 2024, doi: 10.3390/buildings14103147.

[12] S. Ma, Y. Qiao, W. Huang, Z. Wang, Y. Xu, and J. Xie, "A Study on the Diversity and Cultural Characteristics of Decorative Patterns of Traditional Academies in Eastern China Based on Diversity Index and Social Network Analysis," Buildings, vol. 15, no. 5, pp. 692, 2025, doi: 10.3390/buildings15050692.

[13] Y. Song and C. Liao, "Research on the architectural features and artistic elements of traditional buildings in different regions of Jiangxi, China," Buildings, vol. 13, no. 7, pp. 1597, 2023, doi: 10.3390/buildings13071597.

[14] H. A. F. E. Al Dein, "Semiotics as an approach to the analysis of symbolism in islamic architectural arts," Architecture and Engineering, vol. 7, no. 2, pp. 3-19, 2022, doi: 10.23968/2500-0055-2022-7-2-03-19.

[15] Z. Xiong, "Research on the Application of Cultural Symbols and Local Elements in Graphic Design," Frontiers in Art Research, vol. 6, no. 10, pp. 51-57, 2024, doi: 10.25236/FAR.2024.061009.

[16] G. Saypanova, "ETHNOGRAPHY OF PATTERNS: UNDERSTANDING CULTURAL EXPRESSIONS THROUGH DESIGN AND SYMBOLISM," Akademicheckie iccledovaniya v covremennoy nayke, vol. 3, no. 46, pp. 19-22, 2024, doi: 10.5281/zenodo.14227455.

[17] L. Ren, C. Yang, and Z. Zhou, "Cross-Cultural Innovative Ski Wear Design from the Perspective of Cultural Symbol Translation," Textile and Leather Review, vol. 7, pp. 1346-1359, 2024, doi: 10.31881/TLR.2024.161.

[18] T. Cong, Y. Zhang, L. Shen, and R. Cui, "Hidden Messages: Connotation analysis of Textile Trademarks in the Republic of China (1912-1949)," Fibres & Textiles in Eastern Europe, pp. 31(2), 2023, doi: 10.2478/ftee-2023-0016.

[19] J. Ampadu, R. Acquaye, and G. A. Appoh, "Textile design and product innovations from adinkra and bogolanfini ideographic mergers," Journal of Art and Design, vol. 1, no. 1, pp. 28-45, 2022, doi: 10.31586/jad.2022.231.